MICROBIOLOGY

# Skin-specific antibodies neutralizing mycolactone toxin during the spontaneous healing of *Mycobacterium ulcerans* infection

**Mélanie Foulon[1]*, Amélie Pouchin[1]*, Jérémy Manry[2,3]*, Fida Khater[1], Marie Robbe-Saule[1], Amandine Durand[1], Lucille Esnault[1], Yves Delneste[4,5], Pascale Jeannin[4,5], Jean-Paul Saint-André[6], Anne Croué[6], Frederic Altare[7], Laurent Abel[2,3], Alexandre Alcaïs[2,3], Estelle Marion[1†]**



**Buruli ulcer, a neglected tropical infectious disease, is caused by *Mycobacterium ulcerans*. Without treatment, its lesions can progress to chronic skin ulcers, but spontaneous healing is observed in 5% of cases, suggesting the possible establishment of a host strategy counteracting the effects of *M. ulcerans*. We reveal here a skin-specific local humoral signature of the spontaneous healing process, associated with a rise in antibody-producing cells and specific recognition of mycolactone by the mouse IgG2a immunoglobulin subclass. We demonstrate the production of skin-specific antibodies neutralizing the immunomodulatory activity of the mycolactone toxin, and confirm the role of human host machinery in triggering effective local immune responses by the detection of anti-mycolactone antibodies in patients with Buruli ulcer. Our findings pave the way for substantial advances in both the diagnosis and treatment of Buruli ulcer in accordance with the most recent challenges issued by the World Health Organization.**

## INTRODUCTION

Buruli ulcer, a neglected tropical disease caused by *Mycobacterium ulcerans*, is the third most common mycobacterial disease in the world after tuberculosis and leprosy (*1*). This chronic infectious disease is characterized by the destruction of cutaneous tissue, leading to the development of large ulcerative lesions. This tissue destruction is caused by a unique lipid-like toxin called mycolactone, produced by *M. ulcerans*. Mycolactone is cytotoxic at high doses, but, at lower doses, it modulates pain and immune responses, facilitating host colonization (*2*–*6*). Despite this toxin secretion, experimental approaches, supported by observations in human patients, have revealed that immune response modulation by mycolactone is local and regional rather than systemic (*7*, *8*). Moreover, the systemic humoral response to *M. ulcerans* infection is weak (*8*), and *M. ulcerans* is poorly recognized by circulating antibodies (*9*). Histological analyses of patient tissues have shown that Buruli ulcer lesions are surrounded by a massive inflammatory infiltration of leukocytes (*10*). This local infiltration has been characterized in mice and shown to consist predominantly of phagocytes (mostly macrophages and neutrophils) and lymphocytes (*8*). Overall, these findings suggest that the immune response cannot control lesion development, despite the recruitment of several major actors of the immune system. This failure of host immunity is a consequence of the strategy used by *M. ulcerans* to escape the immune system.

The earlier studies described above were performed during the preulcerative and ulcerative phases. No study has ever considered these immune processes during the spontaneous healing stage. Buruli ulcer can be treated with antibiotics during early stages. However, despite the significant improvement of treatments, about 10 to 15% of patients with Buruli ulcer become permanently disabled according to the World Health Organization (*11*–*14*). Furthermore, untreated lesions can spread to entire limbs and progress to chronic skin ulcers (*11*). However, in the absence of medical treatment, spontaneous healing occurs in 5% of cases, as recently reported in Africa and confirmed by the spontaneous healing of untreated Australian patients with *M. ulcerans* infections (*15*, *16*), suggesting the possible establishment of a strategy counteracting the effects of *M. ulcerans* in the host. This observation reveals a role of the host in controlling lesion development. Recent histological studies have shown that B cells accumulate in clusters around sites of *M. ulcerans* infection, suggesting a specific local adaptive response (*10*, *17*). B cells produce immunoglobulin (Ig) and constitute the humoral arm of the immune system. These lymphocytes have both proinflammatory and suppressive roles in the pathophysiology of inflammatory skin disorders (*18*). Furthermore, skin-associated B cells have been shown to be different from lymph node B cells (*19*). This specific local humoral response may enhance local defense and immunity in the context of chronic inflammatory skin diseases (*20*). However, the local antibody-mediated humoral response, to the best of our knowledge, has never been investigated during the course of *M. ulcerans* infection, including the spontaneous healing phase. Using our original mouse model reproducing the key features of the human disease [including spontaneous healing after the ulcerative phase, as previously described by Marion *et al.* (*8*)], we investigated the potential role of natural local antibodies, recognizing the mycolactone produced by *M. ulcerans*. Our findings confirm the presence of these antibodies in humans.

## RESULTS

### Production of skin Igs during *M. ulcerans* infection

We investigated the local humoral response during *M. ulcerans* infection, including the spontaneous healing process, by evaluating Ig gene expression through analyses of mRNA levels in cutaneous

[1]Equipe ATOMycA, U1232 CRCINA, Institut National de la Santé et de la Recherche Médicale (INSERM), Université de Nantes, Université d'Angers, Angers, France. [2]Laboratory of Human Genetics of Infectious Diseases, Necker Branch, Institut National de la Santé et de la Recherche Médicale (INSERM) UMR-1163, Paris, France. [3]Imagine Institute, Paris Descartes-Sorbonne Paris Cité University, Paris, France. [4]Equipe 07, U1232 CRCINA, Institut National de la Santé et de la Recherche Médicale (INSERM), Université de Nantes, Université d'Angers, Angers, France. [5]CHU Angers, Département d'Immunologie et Allergologie, Angers, France. [6]Pathology Department, University Hospital of Angers, 49933 Angers, France. [7]Equipe 05, U1232 CRCINA, Institut National de la Santé et de la Recherche Médicale (INSERM), Université d'Angers, Université de Nantes, Nantes, France.
*These authors contributed equally to this work.
†Corresponding author. Email: estelle.marion@inserm.fr

tissue samples. The FVB/N mouse model (which displays spontaneous healing) was compared with the C57BL/6 mouse (which displays no such healing). Relative mRNA levels for IgM, IgA, and IgG remained stable in both models during early stages of infection (fig. S2). However, the levels of mRNA for all three Ig isotypes increased significantly in FVB/N mice at the ulcerative stage (day 45), reaching a peak during the healing stage (day 75). The levels of mRNA encoding these three isotypes were significantly higher ($P < 0.05$ for IgM and IgG and $P < 0.01$ for IgA, Mann-Whitney $U$ test) in FVB/N mice at the healing stage than in C57BL/6 mice at the necrotic stage. We characterized the Ig profiles of infected tissues by estimating IgM, IgA, and IgG concentrations by enzyme-linked immunosorbent assay (ELISA). Consistent with the mRNA data, total Ig levels increased in the cutaneous tissues of FVB/N mice throughout *M. ulcerans* infection (Fig. 1, A to C). However, despite the absence of clear changes in local levels of Ig mRNA in C57BL/6 mice, we observed an increase in tissue Ig concentration throughout *M. ulcerans* infection in these mice (Fig. 1, A to C). Differences in IgM and IgG concentrations were detected between the two mouse strains. IgG levels in FVB/N mice were twice those in C57BL/6 mice ($P < 0.01$, Mann-Whitney $U$ test) during both the redness and ulcerative stages and were 1.6 times higher ($P < 0.05$, Mann-Whitney $U$ test) during the healing process than during the necrotic stage, whereas IgM levels were higher in C57BL/6 mice from the ulcerative stage (2.7 times higher; $P < 0.01$, Mann-Whitney $U$ test) until necrosis (7.8 times higher; $P < 0.01$, Mann-Whitney $U$ test). These differences, evident from the earliest stages, might reflect high levels of circulating Igs. However, no significant differences in the levels of these Igs were detected between the serum samples of the two mouse strains during the early stages of infection (Fig. 1, D to F). Despite the absence of detectable systemic changes, Ig may accumulate in tissues during inflammation [as recently described (*21*)], potentially accounting for the observed differences between RNA and protein levels. Last, the course of *M. ulcerans* infection is associated with a local humoral response, with the following Ig profiles: IgM > IgG > IgA in C57BL/6 mice and IgG > IgM > IgA in FVB/N mice. There therefore seems to be a specific humoral immunity signature of the healing process, in which IgG predominates.

### Recognition of *M. ulcerans* lysate by local IgG antibodies

Like all mycobacteria, *M. ulcerans* has a large antigenic repertoire [lipoarabinomannan (LAM), surface membrane proteins, and extracellular vesicles] that may trigger the production of specific antibodies by the host (*22*). We therefore investigated the specificity of the local Ig production, by evaluating their ability to recognize *M. ulcerans* whole-cell lysate in ELISA. IgG was the only isotype of Ig able to bind *M. ulcerans* lysate components (fig. S3A). This recognition became stronger with successive stages of infection in both FVB/N and C57BL/6 mice and was maximal during the healing and necrosis stages ($P < 0.01$, Mann-Whitney $U$ test). We then evaluated the ability of IgG subclasses to recognize *M. ulcerans* components (fig. S3B). High levels of IgG1 binding to *M. ulcerans* lysate components were observed in both mouse models. IgG1 binding was detected early in the redness stage in FVB/N mice and later at the edema stage in C57BL/6 mice ($P < 0.01$ for the difference between the two mouse models at the redness stage, Mann-Whitney $U$ test). By contrast, IgG3 recognized *M. ulcerans* lysate components very weakly but similarly in the two mouse strains. The major difference between FVB/N and C57BL/6 mice concerned the IgG2a/b subclasses. IgG2a recognized *M. ulcerans* components at all stages of infection (from the ulcerative to the healing stage) in FVB/N mice but seemed to be absent in C57BL/6 mice. The last subclass, IgG2b, recognized *M. ulcerans* lysate significantly more strongly in C57BL/6 mice, from the ulcerative to the necrotic stage, than in FVB/N mice at equivalent stages ($P < 0.05$, Mann-Whitney $U$ test). In conclusion, local humoral responses differed between FVB/N mice (healing model) and C57BL/6 mice (no spontaneous healing). This difference mostly concerned two specific Ig subclasses: (i) IgG2a, which was produced only in the healing model, and (ii) IgG2b, which recognized *M. ulcerans* components strongly only in the C57BL/6 model. These results suggest a potential role for IgG2a in controlling *M. ulcerans* infection in the FVB/N healing model.

### Recognition of mycolactone by local skin antibodies

The ability of FVB/N mice to heal spontaneously after *M. ulcerans* infection could be explained, in part, by the production of antibodies recognizing the bacterial toxin, mycolactone. We investigated the specificity of these local antibodies for mycolactone in skin tissues by performing ELISA (Fig. 2). IgM produced locally in both mouse strains were unable to recognize mycolactone. IgA, which is known to protect tissues (i.e., epithelial cells) against bacterial toxins (*23*), bound mycolactone at low levels only during the ulcerative stage in FVB/N mice. As observed for *M. ulcerans* lysate, IgG recognized mycolactone at high levels in both mouse models throughout infection. Significantly higher levels of mycolactone recognition by IgG were observed in C57BL/6 mice at the necrotic stage than in FVB/N mice at the healing stage ($P < 0.05$, Mann-Whitney $U$ test). We then analyzed IgG subtypes at each stage of infection. From the edema stage to the ulcerative stage, IgG1 appeared to be a subclass able to bind mycolactone at higher levels in FVB/N mice than in C57BL/6, whereas IgG2b seemed to recognize mycolactone at higher levels and from earlier stages exclusively in C57BL/6 mice ($P < 0.01$ for IgG1 in FVB/N versus C57BL/6 mice and $P < 0.01$ for IgG2b in the ulcerative stage in C57BL/6 mice relative to FVB/N mice, Mann-Whitney $U$ test). During the last stage of infection (necrosis versus healing), same observations were made ($P < 0.05$ versus FVB/N mice, Mann-Whitney $U$ test). The mycolactone-binding profile of IgG3 was similar in both mouse models. Last, as for the recognition of *M. ulcerans* lysate, the major difference concerned the IgG2a subclass, which appeared to be specific to FVB/N mice. This subclass bound the toxin from the ulcerative stage to the healing stage. The lack of IgG2a detection in assays performed on C57BL/6 mice may be explained by a mutation of the IgG2a gene in these mice (*24*). We performed assays in another mouse model displaying no spontaneous healing (BALB/c mice), in which the IgG2a gene is present and functional, to exclude the possibility of exclusion of a strain-specific phenotype and confirm the importance of this protein in the healing process and in mycolactone binding. The IgG2a antibody produced by BALB/c mice did not recognize mycolactone (see fig. S4). Together, these results reveal the existence of different mycolactone recognition profiles between mouse models of healing and necrotic infection. IgG2b appears to be a specific subclass capable of recognizing *M. ulcerans* toxin in C57BL/6 mice, but it is unable to control infection efficiently. By contrast, IgG2a was specific to the spontaneous healing model (FVB/N mice) and may be involved in the control of *M. ulcerans* infection associated with spontaneous healing.

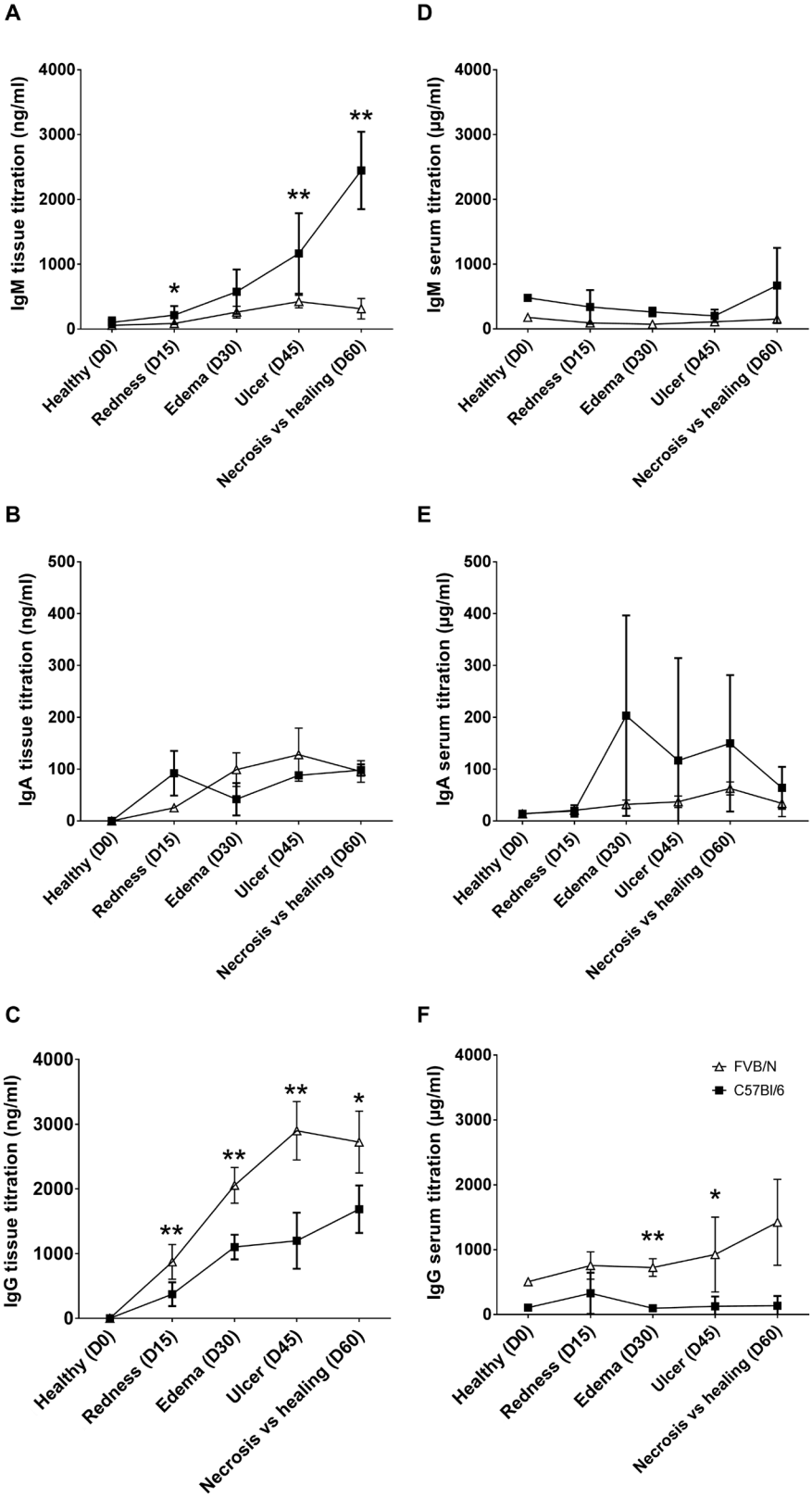


**Fig. 1. Quantification of IgM, IgA, and IgG in cutaneous tissues at the site of inoculation and in serum.** Kinetics of Ig production, after inoculation with viable *M. ulcerans* bacilli, evaluated by quantitative ELISA. (**A** to **C**) Cutaneous tissue samples ($n = 5$ for each strain), for which protein concentrations were normalized, and (**D** to **F**) serum samples ($n = 5$ for each strain). The histograms show the means ± SD. *$P < 0.05$ and **$P < 0.01$ (comparison of Ig titration in FVB/N and C57BL/6 mice at each stage of the disease; Mann Whitney *U* tests).

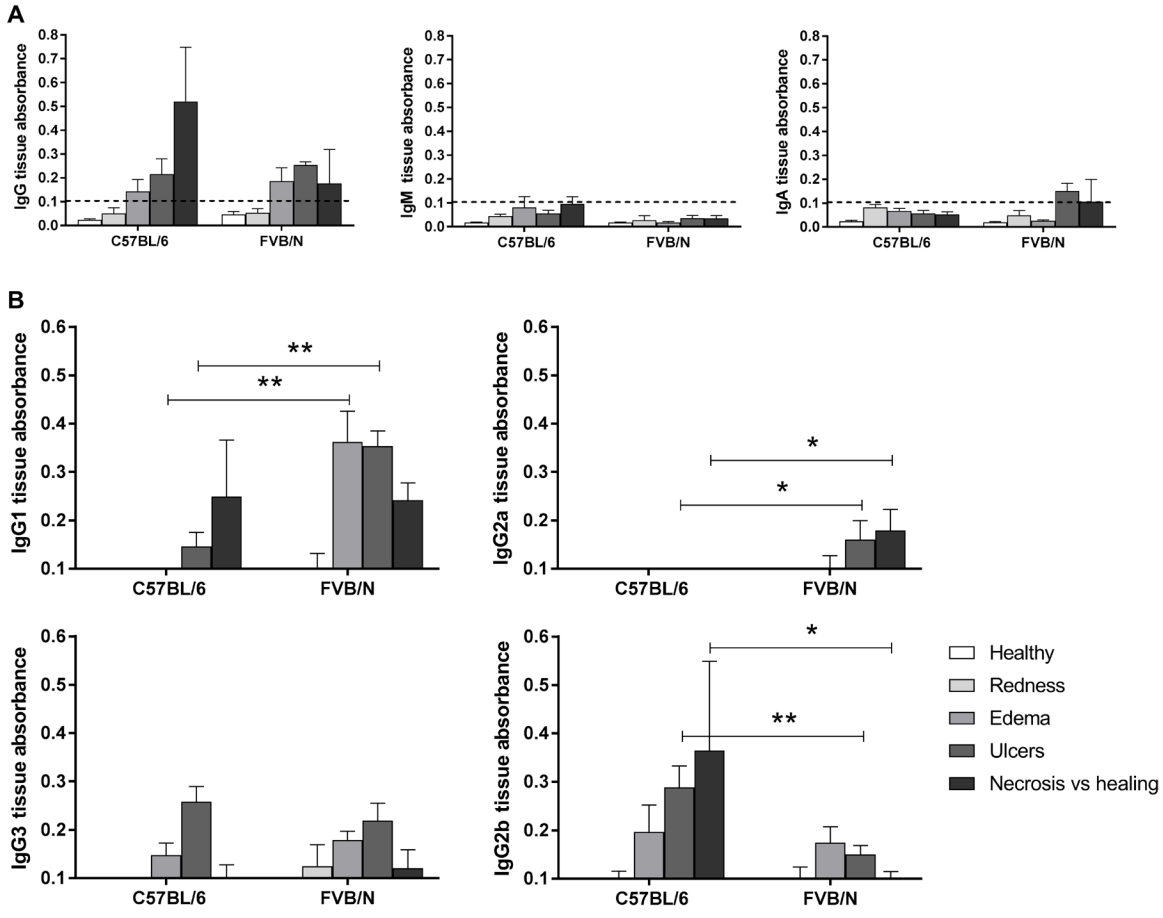


**Fig. 2. Detection of cutaneous IgG binding to mycolactone by quantitative ELISA.** Each well of an ELISA MaxiSorp plate was coated with 3 ng of mycolactone, and the Ig concentrations of cutaneous tissue samples were normalized before their addition to the plate. Antibodies binding to mycolactone on the plate were recognized by horseradish peroxidase (HRP)–conjugated secondary antibodies. (**A**) Detection of IgG, IgM, and IgA and (**B**) IgG1, IgG2a, IgG3, and IgG2b recognizing the mycolactone in cutaneous tissue from FVB/N and C57BL/6 mice at various stages of infection (healthy, redness, ulcer, necrosis, or healing) ($n = 3$ to 5 mice per mouse strain). The detection limit was an absorbance of 0.1. The histograms show the means ± SD. *$P < 0.5$, **$P < 0.01$ (Mann-Whitney $U$ test).

## Neutralization of mycolactone by antibodies present in the skin

We investigated the ability of these antibodies to recognize and neutralize mycolactone, by assessing their capacity to neutralize the immunomodulatory properties of the toxin. Mycolactone is known to inhibit the production of inflammatory cytokines by binding to the Sec61 translocon (*25*). We based our neutralization test on this effect and therefore incubated stimulated T lymphocytes (cytokine-producing cell model used here as a readout tool) with mycolactone alone or with mycolactone previously incubated with IgG purified from the skin of FVB/N and C57BL/6 mice and then compared interleukin-2 (IL-2) and interferon-γ (IFN-γ) production after 6 hours. Contact between T cells and the toxin greatly decreased IL-2 and IFN-γ production levels relative to the positive control (stimulated T cells alone) in both mouse models (Fig. 3). By contrast, the production of these two cytokines was similar to the positive control for T cells in contact with mycolactone previously incubated with IgG purified from the skin of FVB/N mice but not for T cells in contact with mycolactone previously incubated with IgG purified from C57BL/6 mice. Thus, the IgG produced in the skin of FVB/N mice during the healing stage can neutralize the *M. ulcerans* toxin. This neutralization may be involved in the healing process.

## Local emergence of antibody-producing cells during *M. ulcerans* infection

On the basis of the hypothesis of a local humoral immune response being established during spontaneous healing, we assessed the physiological relevance of this process by investigating the presence of antibody-producing B cells in vivo. We used four-color staining to analyze B cell populations from FVB/N mice and identified three populations: (P1) cells with a $CD45^+$, $CD19^+$, $B220^+$ phenotype corresponding to B cells; (P2) $CD45^+$, $CD19^+$, $B220^{int}$ cells corresponding to plasmablasts; and (P3) $CD45^+$, $CD19^-$, $B220^{int}$, $CD138^+$ cells, corresponding to the murine markers of the last stage of B cell maturation, plasma cells (*26*). The frequency of lymphoid cells ($CD45^+$) increased 37-fold relative to control skin during the spontaneous healing process (Fig. 4A). Consequently, the total number of B cells increased, but the proportions of the various subsets remained constant. The only change observed was an increase in the proportion of total lymphoid cells accounted for by the plasma cell subset, which increased from 0.04 to 0.63% (corresponding to an increase of 43 to 19,732 plasma cells/g of skin) during the first few steps of the spontaneous healing process (day 55), whereas no such increase was observed in uninfected skin (control), as shown in Fig. 4C. The presence of this specific B cell subtype was confirmed by histological analysis (Fig. 4B).

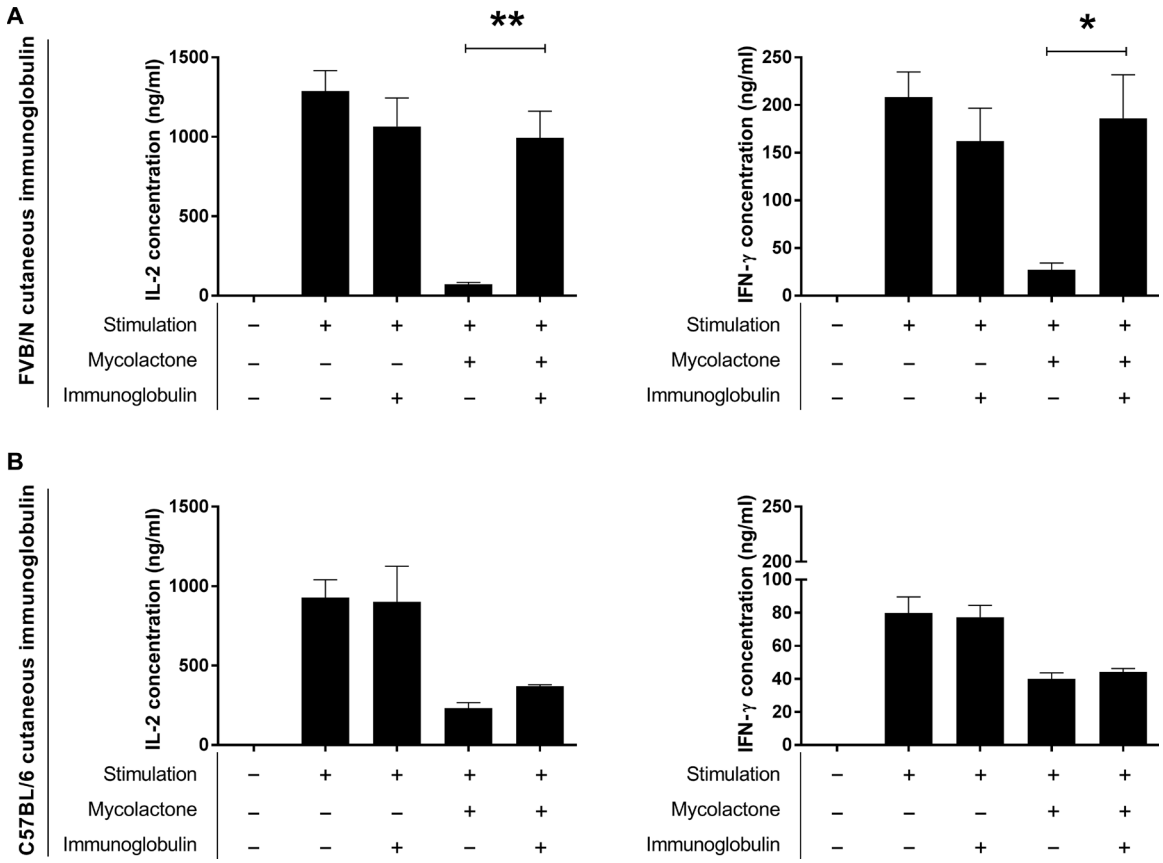


**Fig. 3. Neutralization of mycolactone by cutaneous Ig from FVB/N mice infected with *M. ulcerans*.** $CD4^+$ lymphocytes were stimulated with phorbol 12-myristate 13-acetate/ionomycin. Mycolactone was used at a concentration of 4 ng/ml. Igs purified from the skin of (**A**) FVB/N mice or (**B**) C57BL/6 mice infected with *M. ulcerans* were used at a ratio of 10 Ig molecules per molecule of mycolactone. Left: IL-2 quantification; right: IFN-γ quantification. The data shown correspond to one experiment performed in triplicate (means ± SD). *$P < 0.05$ and **$P < 0.01$ (Student's *t* test).

The proportion of B1-like B cells ($CD45^+$, $CD19^+$, $B220^{int}$, $CD43^+$), a specific subset that has been shown to produce antibodies specifically in the skin (*27*), increased during spontaneous healing, reaching 0.07% of total lymphoid cells (see fig. S5). The proportion of these antibody-producing cells decreased when the lesion appears to be completely healed (day 75) but remained higher than that in control skin. Our results thus show that the number of antibody-producing cells strongly increase in the skin during the spontaneous healing process, supporting a role for the local humoral response in this phenomenon, through the production of anti-mycolactone antibodies.

### Recognition of mycolactone by local IgG purified from skin biopsy specimens from patients with Buruli ulcer

In addition to this detailed characterization of anti-mycolactone Igs in mice, we also assessed the levels of these IgGs in patients with Buruli ulcer. We used ELISA to detect anti-mycolactone antibodies in skin samples from patients (with or without a diagnosis of Buruli ulcer) provided by the Centre de Diagnostic et de Traitement de la Lèpre et de l'Ulcère de Buruli (CDTLUB) of Pobé (Benin). In 73% of patients with polymerase chain reaction (PCR)–confirmed Buruli ulcer, the most severe form of the disease had been diagnosed: an ulcerative lesion (which may be associated with other forms, such as edema or plaques). Mycolactone was recognized by local antibodies recovered from the lesions of 60% of patients with PCR-confirmed Buruli ulcer (9 of 15) (all presenting an ulcer), whereas mycolactone was detected in only one biopsy specimen from the control patients (not diagnosed with Buruli ulcer; $P < 0.05$, Mann-Whitney *U* test; Fig. 5). This particular patient has since developed squamous cell carcinoma, a disease that is known to occur after Buruli ulcer lesions in some cases (*27*, *28*). We cannot, therefore, exclude the possibility that this patient may have already had a lesion due to *M. ulcerans* infection. Last, there may be several reasons for the lack of mycolactone-binding IgG detection in 40% of patients with PCR-confirmed Buruli ulcer (6 of 15) such as lesion type, the sampling site (distance from the site of infection), and the treatment duration. Last, we provide here the first demonstration that the human organism can generate an effective humoral response involving the production of antibodies recognizing mycolactone during *M. ulcerans* infection.

## DISCUSSION

Buruli ulcer is a neglected tropical disease that remains the third most common mycobacterial disease worldwide. This debilitating skin disease is caused by *M. ulcerans*, which produces a lipid-like toxin, mycolactone, the main virulence factor of the bacillus. Without treatment, lesions can progress to chronic skin ulcers. However, these severe lesions may heal spontaneously, as observed in 5% of cases, suggesting that mechanisms for counteracting the effects of *M. ulcerans* may develop in the host. Despite the development of animal models, the mechanisms of the spontaneous healing process remain unclear. We previously showed (i) the absence of a systemic immune cell response signature and (ii) a weak involvement of the

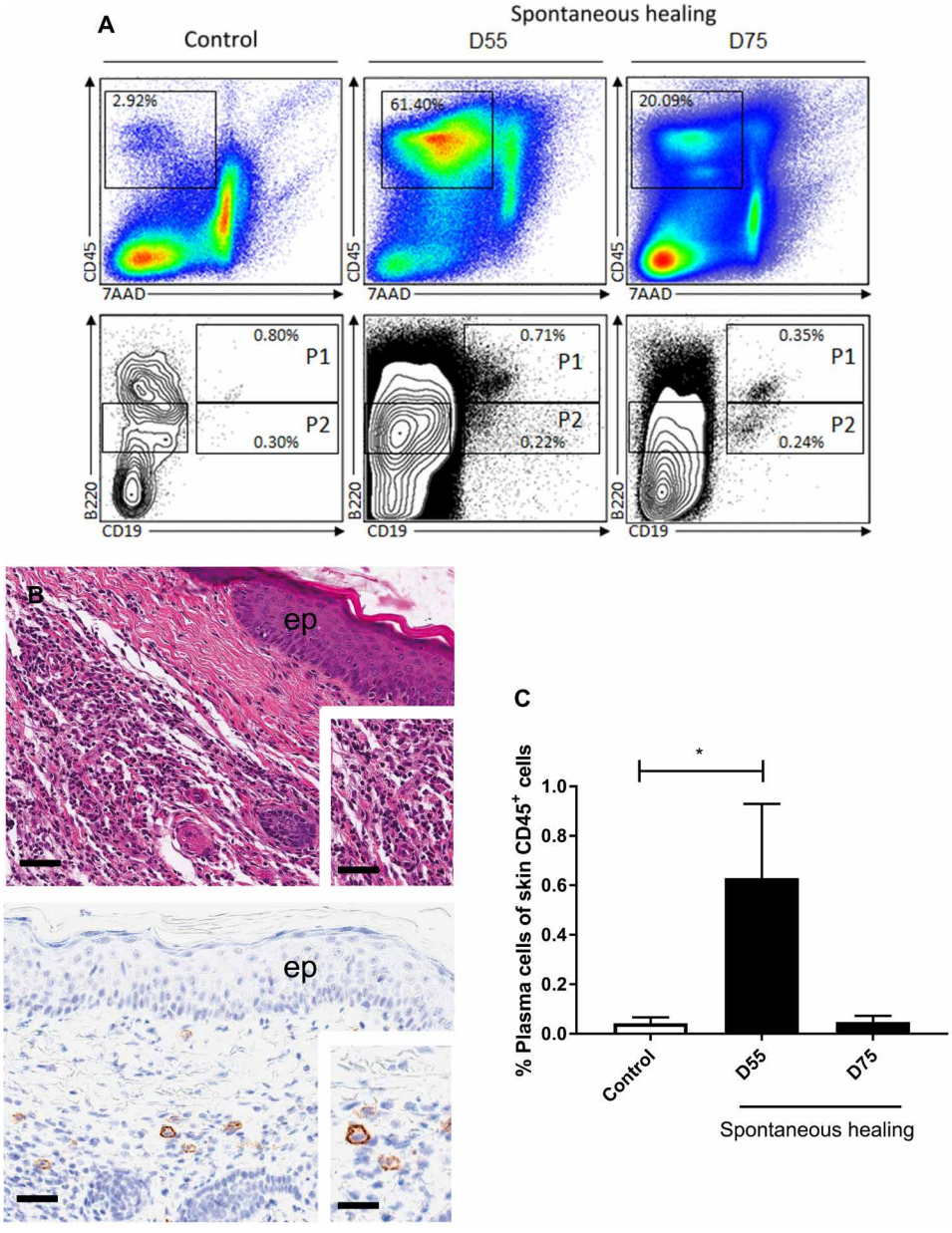


**Fig. 4. Emergence of plasma cells (CD138$^+$) in the skin during *M. ulcerans* infection in the FVB/N mouse model of spontaneous healing.** (**A**) Cells were analyzed by four-color flow cytometry with the specific staining of total lymphoid cells (CD45$^+$), B cells (population P1 = CD45$^+$, CD19$^+$, B220$^+$), plasmablasts (population P2 = CD45$^+$, CD19$^+$, B220$^{int}$), and plasma cells (CD45$^+$, CD19$^-$, B220$^{int}$, CD138$^+$). The results shown here are from one representative experiment performed in duplicate. (**B**) Local inflammatory infiltration (inset) in the dermis of *M. ulcerans* infected mice at the ulcerative stage, typical of *M. ulcerans* infection. ep, epidermis. Immunostaining showing CD138$^+$ plasma cells (activated B cells able to produce antibodies) in the dermis. (**C**) Flow cytometry analysis showing the emergence of plasma cells (CD45$^+$, CD19$^-$, B220$^{int}$, CD138$^+$) during the early steps of the spontaneous healing process (the control is uninfected skin). The histograms show the means ± SD. *$P < 0.05$ (Student's *t* test). Scale bars, 160 μm (B top), 80 μm (B, top, inset), 100 μm (B bottom) and 20 μm (B bottom, inset).

local cellular immune response in the switch from acute to chronic infection (*8*). These results highlight the local consequences of the disease, as observed with other approaches (*7*, *29*). Recent histological studies have shown that B cells accumulate in clusters around the site of *M. ulcerans* infection (*10*). B cell infiltrates have been observed under chronic inflammatory skin conditions, including cutaneous leishmaniasis and atopic dermatitis (*30*, *31*). The debate about the pro- or anti-inflammatory role of skin B cells continues, but these cells have been shown to be involved in the resolution of skin inflammation in a mouse model of psoriasis-like inflammation (*32*). Furthermore, in addition to producing antibodies locally, B cells have been shown to play a role in the process of wound healing (*33*).

In this context, we used our mouse model of spontaneous healing to investigate the humoral response at all stages of *M. ulcerans* infection, including spontaneous healing. We demonstrated the presence of antibody-producing B cells during infection and their increase in number during infection, peaking during the early stages of spontaneous healing (the transition from ulceration to healing).

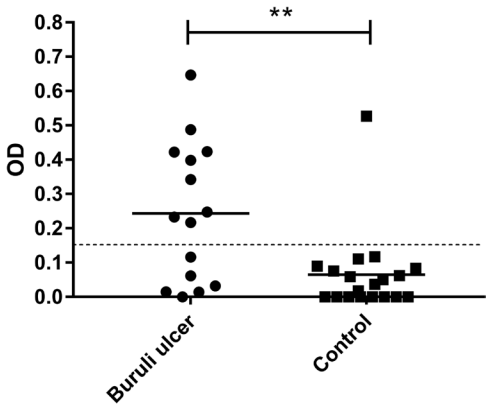


**Fig. 5. Detection of cutaneous Igs binding to mycolactone in the lesions of patients diagnosed with Buruli ulcer.** Wells were coated with mycolactone, and antibodies binding to mycolactone in the plate were recognized by HRP-conjugated secondary antibodies. Biopsy specimens from patients with suspected and/or PCR-confirmed Buruli ulcer were provided by the CDTUB of Pobè (Benin). In PCR-confirmed Buruli ulcer patients, biopsies were performed on active lesions. It was not, therefore, possible to identify the patients subsequently displaying spontaneous healing. The detection limit was an absorbance of 0.150. $^{**}P < 0.05$ (Mann Whitney *U* test). Buruli ulcer group, $n = 15$; control group, $n = 19$. OD, optical density.

We detected Igs able to recognize the lipid toxin of *M. ulcerans*, mycolactone, at all stages of infection. These Igs were found in the skin of infected mice but not in their sera. We also provide the first demonstration of the presence of these Igs in biopsy specimens from patients with Buruli ulcer. No anti-mycolactone antibodies have ever been detected in serum from patients. Collectively, these results highlight the existence of a distinct humoral signature in response to *M. ulcerans* infection, with the skin-specific production of antibodies against mycolactone.

It seems likely that the spontaneous healing observed in FVB/N mice is triggered by host genetic factors. In particular, FVB/N mice present modifications of two elements involved in the immune response: (i) a deficiency in the secretion of complement component 5 and (ii) an NLRP polymorphism. However, we have previously observed that the AKR mice, which harbor the first of these modifications, (data not shown) and the BALB/c mice (*8*), which harbor the second mutation, have features similar to C57BL/6 mice, with no spontaneous healing. This led us to investigate the involvement of the antibody-mediated immune response in the spontaneous healing process. The specific Igs produced locally and able to recognize *M. ulcerans* components, including mycolactone in particular, may contribute to the control of infection observed during spontaneous healing. We investigated this possibility, by evaluating the ability of IgG subclasses to recognize *M. ulcerans* components. We tagged a specific subclass of Ig, IgG2a, which is known to diffuse readily in the skin (*23*). This subclass has been reported to be highly effective at neutralizing bacterial exotoxins, such as diphtheria toxin, enterotoxin B, and *Bacillus anthracis*–associated toxin (*34*), was produced only in the spontaneous healing model, and seems to be the signature of this model in terms of mycolactone recognition. We also found that the IgG recognizing *M. ulcerans* components that were isolated from the skin of FVB/N mice was able to neutralize the toxic activity of mycolactone. No other mycolactone-neutralizing antibodies have been identified in any other mouse model.

The neutralization of bacterial toxins is an important part of the humoral immune response to bacterial infections (*34*). Our results therefore suggest that mycolactone neutralization may be the key to the spontaneous healing process of Buruli ulcer. We have previously demonstrated that the tissue environment in FVB/N mice during spontaneous healing induced a switch to lower production of mycolactone by *M. ulcerans*, despite similar bacterial loads. This switch could probably be at the origin of the ability of skin antibodies to neutralize the remaining mycolactone, leading to the control of the acute inflammatory response and the improvement of tissue repair, as we previously observed (*8*). Last, the neutralization phenomenon may block mycolactone activity in various ways: It would probably be more difficult for mycolactone linked to an antibody to gain access to or inhibit known intracellular targets, such as the Sec61 translocon, (i) if the antibody-mycolactone complex cannot cross membranes or (ii) if the antibody hampers the binding of the mycolactone. It is therefore reasonable to assume that (iii) neutralizing antibodies may help to eliminate the toxin by targeting them to phagocytic cells.

The existence of anti-mycolactone antibodies opens up exciting new perspectives for innovations in diagnosis, treatment, and vaccine development responding to the scientific challenge issued by the World Health Organization. There is currently no simple diagnostic tool suitable for use in the rural areas of developing countries. This situation is particularly regrettable, as the early stages of Buruli ulcer can be treated locally, whereas the treatment of later stages requires extensive surgery in larger hospitals, with longer periods of hospitalization, at much greater expense. The development of a new diagnostic tool, such as a test based on monoclonal antibody production, might be more appropriate for these endemic regions. In addition, extrapolating from the use of neutralizing antibodies to broaden the treatment spectrum for toxic venoms, mycolactone-neutralizing antibodies might also be potentially useful in strategies for treating Buruli ulcer.

## MATERIALS AND METHODS

### Ethics statement for animal experiments and use of human tissues

All animal experiments were performed in accordance with national guidelines (articles R214-87 to R214-90 of the French "rural code") and European guidelines (directive 2010/63/EU of the European Parliament and of the Council of 2010 September 22 on the protection of animal used for scientific purposes). All protocols were approved by the ethics committee of the Pays de la Loire region, under protocol no. APAFIS8904. Mice were housed under specific pathogen-free conditions in the animal house of the Angers University Hospital, France (agreement A 49 007 002). The use of biopsy samples from patients for research purposes was approved by the research committee of government of Benin (Ministry of Health, Republic of Benin, agreement number 2893).

### *M. ulcerans* strain and inoculation

*M. ulcerans* strain 01G897 was originally isolated from patients from French Guiana by the bacteriology team of Angers Hospital (*35*) and stored in our laboratory since this time. A bacterial suspension was prepared, as previously described (*8*, *22*), and its concentration was adjusted to $2 \times 10^5$ acid-fast bacilli/ml for an inoculation of $1 \times 10^4$ bacilli in 50 µl into the tails of 6-week-old female consanguineous C57BL/6 and FVB/N mice (Janvier, Le Genest Saint Isle, France) and BALB/c mice (Charles River Laboratories, Saint-Germain-Nuelles, France).

### Mycolactone

The Malaysian *M. ulcerans* 1615 strain was originally isolated from human skin biopsy from Malaysia (*36*) and given by P. Small laboratory in 2005. The strain was cultured on solid 7H10 medium supplemented with 10% OADC (oleic acid, dextrose, catalase; Difco, Becton-Dickinson) at 30°C for 45 days. Mycolactone A/B was then purified from whole bacteria, as previously described (*37*). Mycolactone was diluted to a concentration of 3 mg/ml in absolute ethanol and stored in the dark in amber glass tubes at −20°C.

### Mouse tissue preparation and serum sampling

Skin samples from infected mice with visible lesions (displaying redness, edema, ulcer, necrosis, or healing) were excised (we removed 1 cm of cutaneous tissue from around the lesion) and crushed in phosphate-buffered saline (PBS) supplemented with cOmplete EDTA-free cocktail (Roche), with a TissueRuptor (QIAGEN). The resulting suspensions were centrifuged at 3500*g* for 10 min at 4°C. The supernatants were stored at −80°C. Blood samples were collected by retro-orbital puncture at each clinical stage of infection before tail excision. The blood was centrifuged at 1500*g* for 10 min to isolate serum, which was recovered and stored at −80°C.

### Preparation of human biopsy tissues

Skin biopsy specimens were provided by the Centre de Diagnostic et de Traitement de la Lèpre et de l'Ulcère de Buruli (CDTLUB) of Pobé (Benin). The biopsy specimens were crushed in PBS supplemented with protease inhibitors (cOmplete EDTA-free cocktail, Roche), with a TissueRuptor (QIAGEN), as described for mouse tissues. The resulting suspensions were centrifuged at 3500*g* for 10 min at 4°C. The resulting supernatants were stored at −80°C.

### Quantitative PCR analysis

Tail skins from infected mice were excised and immediately placed into RNAlater (QIAGEN) and stored at −20°C. Skin tissues were crushed and homogenized with a TissueRuptor (QIAGEN), and total RNA was then purified with the RNeasy fibrous tissue midi kit (QIAGEN). The first-strand complementary DNA was synthesized from 750 ng of RNA with the M-MLV reverse transcriptase (Invitrogen). Quantitative PCR was performed to quantify the levels of IgM, IgA, and IgG mRNA. Specific gene expression was calculated by the relative expression method (using actin as the calibrator). The sequences of the primers and probes used are provided in table S1.

### Quantification of proteins and Igs

Total protein levels were determined with a colorimetric assay (Protein Assay Dye Reagent), according to the manufacturer's instructions, with Dye Reagent Concentrate Refill (5000006, Bio-Rad) and a standard curve (bovine gamma globulin, kit 1, 50000001, Bio-Rad). Mouse tissue samples were normalized to identical protein concentrations before testing. IgA, IgM, and IgG were quantified in crushed tissue samples and mouse sera by ELISA kit from eBioscience, according to the manufacturer's recommendations (Mouse IgA Ready-SET-Go, 88-50450; Mouse IgM Ready-SET-Go, 88-50470; Mouse IgG Ready-SET-Go, 88-50400).

### Ig purification

Tail skins from infected mice were excised and crushed with metallic beads and a TissueRuptor (QIAGEN) in an equal volume of PBS supplemented with proteases inhibitor (cOmplete EDTA-free cocktail, Roche) and protein A/G IgG Binding Buffer (Thermo Fisher Scientific). The resulting suspensions were centrifuged at 8000*g* for 45 min at 4°C. Ig were then purified with a NAb protein A/G spin column (Thermo Fisher Scientific), followed by a NAb protein L spin column (Thermo Fisher Scientific), according to the manufacturer's instructions.

### Detection of antibodies directed against *M. ulcerans* lysate by ELISA

*M. ulcerans* strain 01G897 lysate was prepared as previously described (*8*). *M. ulcerans* lysate (0.5 µg), diluted in 100 µl of sodium bicarbonate buffer [50 mM (pH 9.6)], was immobilized in 96-well ELISA plates (Nunc-Immuno Plates, MaxiSorp 456537, Thermo Fisher Scientific) by overnight incubation at 4°C. The coated plates were washed four times with 0.05% Tween 20 in PBS and were then saturated by incubation with 5% skimmed milk powder in PBS for 2 hours at room temperature. The plates were washed a further four times and were then incubated with crushed tissue samples with normalized protein contents in 1% skimmed milk powder in PBS for 2 hours at room temperature. After four washes, antibodies directed against *M. ulcerans* lysate were detected with horseradish peroxidase (HRP)–conjugated secondary antibodies diluted 1:500 in 1% skimmed milk powder in PBS. The plates were incubated with the secondary antibodies (table S1) for 1 hour at room temperature and were then washed four times. The KPL SureBlue TMB Microwell Peroxidase Substrate was used for secondary antibody detection, and 1 M $H_2SO_4$ was added to stop the reaction. Absorbance was measured at $\lambda = 450$ nm (with a reference at $\lambda = 570$ nm) (Multiskan Ascent, Thermo Fisher Scientific); results are expressed in optical density units.

### Detection of mycolactone-binding antibodies

ELISA was performed to detect antibodies directed against mycolactone present in human tissues, mouse cutaneous tissues, and mouse sera. Mycolactone A/B (3 ng) in absolute ethanol was immobilized in 96-well plates (Nunc-Immuno Plates, MaxiSorp 456537, Thermo Fisher Scientific) by evaporating off the ethanol for approximately 2 hours in the dark; coated plates were stored at −20°C in the dark for several weeks. They were incubated overnight at 4°C with 5% skimmed milk powder in PBS. The protein concentrations of mouse tissue samples were normalized, mouse serum samples were diluted 10-fold, and human samples were diluted twofold. The plates were washed three times in 0.05% Tween 20 in PBS and were then incubated with diluted samples for 2 hours at room temperature. The plates were washed four times and incubated with HRP-conjugated secondary antibodies [goat anti-mouse IgG1, goat anti-mouse IgG2a, goat anti-mouse IgG2b, goat anti-mouse IgG3, and goat anti-mouse IgG/IgA/IgM (H + L)] (diluted 1:1000 in 1% skimmed milk in PBS for 2 hours at room temperature) (table S1). Bound antibodies were revealed using the SureBlue TMB Microwell Peroxidase Substrate (KPL) used for secondary antibody detection, and 1 M $H_2SO_4$ was added to stop the reaction. Absorbance was measured at 450 nm and was expressed in optical density units.

### Neutralizing activity assay

$CD4^+$ T cells were isolated from the spleens of C57BL/6 mice by magnetic sorting (MACS technology kit 130-104-454), according to the manufacturer's instructions (Miltenyi Biotec). The purity of $CD4^+$ T cell preparations was determined by flow cytometry, with phycoerythrin-conjugated anti-CD4 monoclonal antibody (eBioscience) and fluorescein isothiocyanate–conjugated anti-CD3ε monoclonal antibody (eBioscience). $CD4^+$ T cells (200,000 cells per

well; 100 µl per well) were used to seed 96-well plates. Purified IgG from infected tissue of five mice was diluted in RPMI 1640 (Lonza) supplemented with 10% fetal calf serum (Eurobio), 2 mM glutamine, streptomycin (10 U/ml), and penicillin (100 U/ml) (Lonza). Under some conditions, these were mixed with mycolactone A/B (8 ng/ml) in a 10:1 ratio in a tube and incubated at 37°C with continuous stirring for 45 min. Fetal calf serum was added to the preparation at a final concentration of 10%, followed by phorbol 12-myristate 13-acetate (10 ng/ml) and 1 nM ionomycin. This preparation (100 µl per well) was then added to $CD4^+$ T cells. Cells were incubated for 6 hours at 37°C under an atmosphere containing 5% $CO_2$, and supernatants were collected and stored at −20°C. IL-2 and IFN-γ were quantified by ELISA (eBioscience), according to the manufacturer's instructions (mouse IL-2 Ready-SET-Go, 88-7024; mouse IFN-γ Ready-SET-Go, 88-7314).

### Immune cell isolation and flow cytometry analysis

Tail skin was excised from three mice. Tissues were digested with the Multi Tissue Dissociation kit 1 from Miltenyi Biotec (reference 130-110-201), according to the manufacturer's instructions. A four-color staining method was used to identify B cell subsets: $CD45^+$, $CD19^+$, $B220^+$, and $CD138^+$ cells were labeled with APC (allophycocyanin) cyanidine7 anti-CD45 (BD Biosciences), phycoerythrin anti-CD19 (BD Biosciences), [phycoerythrin-cyanidine7] anti-CD45R/B220 (BD Biosciences), and BB515 anti-CD138 (BD Biosciences) antibodies; dead cells were excluded from the analysis by staining with 7AAD (7-amino actinomycin D) (Miltenyi Biotec). Flow cytometry analysis was performed on a MACSQuant analyzer. Results were analyzed with FlowLogic software.

### Immunohistology

Tails from infected mice were excised and immediately fixed by incubation in 4% paraformaldehyde for 24 hours. Tissues were then embedded in paraffin and cut into 5-mm-thick sections. Hematoxylin phloxine saffron staining was performed according to the manufacturer's protocol. Immunohistochemical staining was performed with an anti-CD138 polyclonal antibody (Thermo Fisher Scientific ref. no. 36-2900) diluted 1:250 according to the manufacturer's protocol.

### Statistical analysis

The data, presented as means and SE, were analyzed with GraphPad Prism 5.0 software (GraphPad Software, San Diego, CA, USA). Different pathological stages in each mouse strain were compared in Kruskal-Wallis tests with Dunn's multiple comparison test. FVB/N and C57BL/6 (as well as BALB/c for the ulcerative stage) mice were compared, at each clinical stage, with Mann-Whitney *U* tests. Patients with buruli ulcer and controls were analyzed in Mann-Whitney *U* tests. A Student's *t* test was used to compare flow cytometry data.

## SUPPLEMENTARY MATERIALS

Supplementary material for this article is available at http://advances.sciencemag.org/cgi/content/full/6/9/eaax7781/DC1

Supplementary Materials and Methods

Table S1. HRP-conjugated secondary antibodies used in this study.

Table S2. Primer sequences used in this study.

Fig. S1. Macroscopic appearance of lesions in FVB/N and C57BL/6 mice infected with *M. ulcerans*.

Fig. S2. Ig gene expression in the cutaneous tissues of mice during the course of *M. ulcerans* infection.

Fig. S3. Detection of cutaneous IgG binding to *M. ulcerans* lysate by quantitative ELISA.

Fig. S4. Cutaneous IgG2a and IgG2b binding mycolactone from C57BL/6, FVB/N, and BALB/c mice at the ulcerative stage.

Fig. S5. Quantification of local B1-like subset of B cells in the skin during *M. ulcerans* infection.

Fig. S6. Markers of murine B cell subsets used for flow cytometry analysis.

References (*38*, *39*)

## REFERENCES AND NOTES


1. F. Portaels, M. T. Silva, W. M. Meyers, Buruli ulcer. *Clin. Dermatol.* **27**, 291–305 (2009).
2. E. Marion, O. R. Song, T. Christophe, J. Babonneau, D. Fenistein, J. Eyer, F. Letournel, D. Henrion, N. Clere, V. Paille, N. C. Guérineau, J. P. Saint André, P. Gersbach, K. H. Altmann, T. P. Stinear, Y. Comoglio, G. Sandoz, L. Preisser, Y. Delneste, E. Yeramian, L. Marsollier, P. Brodin, Mycobacterial toxin induces analgesia in buruli ulcer by targeting the angiotensin pathways. *Cell* **157**, 1565–1576 (2014).
3. C. Demangel, T. P. Stinear, S. T. Cole, Buruli ulcer: Reductive evolution enhances pathogenicity of *Mycobacterium ulcerans*. *Nat. Rev. Microbiol.* **7**, 50–60 (2009).
4. L. Marsollier, J. Aubry, E. Coutanceau, J. P. S. André, P. L. Small, G. Milon, P. Legras, S. Guadagnini, B. Carbonnelle, S. T. Cole, Colonization of the salivary glands of *Naucoris cimicoides* by *Mycobacterium ulcerans* requires host plasmatocytes and a macrolide toxin, mycolactone. *Cell. Microbiol.* **7**, 935–943 (2005).
5. L. Mosi, N. K. Mutoji, F. A. Basile, R. Donnell, K. L. Jackson, T. Spangenberg, Y. Kishi, D. G. Ennis, P. L. C. Small, *Mycobacterium ulcerans* causes minimal pathogenesis and colonization in medaka (*Oryzias latipes*): An experimental fish model of disease transmission. *Microbes Infect.* **14**, 719–729 (2012).
6. R. E. Simmonds, F. V. Lali, T. Smallie, P. L. Small, B. M. Foxwell, Mycolactone inhibits monocyte cytokine production by a posttranscriptional mechanism. *J. Immunol.* **182**, 2194–2202 (2009).
7. A. G. Fraga, A. Cruz, T. G. Martins, E. Torrado, M. Saraiva, D. R. Pereira, W. M. Meyers, F. Portaels, M. T. Silva, A. G. Castro, J. Pedrosa, Mycobacterium ulcerans triggers T-cell immunity followed by local and regional but not systemic immunosuppression. *Infect. Immun.* **79**, 421–430 (2010).
8. E. Marion, U. Jarry, C. Cano, C. Savary, C. Beauvillain, M. Robbe-Saule, L. Preisser, F. Altare, Y. Delneste, P. Jeannin, L. Marsollier, FVB/N mice spontaneously heal ulcerative lesions induced by *Mycobacterium ulcerans* and switch *M. ulcerans* into a low mycolactone producer. *J. Immunol.* **196**, 2690–2698 (2016).
9. K. M. Dobos, E. A. Spotts, B. J. Marston, C. R. Horsburgh Jr., C. H. King, Serologic response to culture filtrate antigens of *Mycobacterium ulcerans* during Buruli ulcer disease. *Emerg. Infect. Dis.* **6**, 158–164 (2000).
10. M. T. Ruf, C. Steffen, M. Bolz, P. Schmid, G. Pluschke, Infiltrating leukocytes surround early Buruli ulcer lesions, but are unable to reach the mycolactone producing mycobacteria. *Virulence* **8**, 1918–1926 (2017).
11. Q. B. Vincent, M. F. Ardant, A. Adeye, A. Goundote, J. P. Saint-André, J. Cottin, M. Kempf, D. Agossadou, C. Johnson, L. Abel, L. Marsollier, A. Chauty, A. Alcaïs, Clinical epidemiology of laboratory-confirmed Buruli ulcer in Benin: A cohort study. *Lancet Glob. Health* **2**, e422–e430 (2014).
12. D. M. Phanzu, P. Suykerbuyk, D. B. B. Imposo, P. N. Lukanu, J. B. M. Minuku, L. F. Lehman, P. Saunderson, B. C. de Jong, P. T. Lutumba, F. Portaels, M. Boelaert, Effect of a control project on clinical profiles and outcomes in buruli ulcer: A before/after study in Bas-Congo, Democratic Republic of Congo. *PLOS Negl. Trop. Dis.* **5**, e1402 (2011).
13. A. C. Wadagni, Y. T. Barogui, R. C. Johnson, G. E. Sopoh, D. Affolabi, T. S. van der Werf, J. de Zeeuw, J. Kleinnijenhuis, Y. Stienstra, Delayed versus standard assessment for excision surgery in patients with Buruli ulcer in Benin: A randomised controlled trial. *Lancet Infect. Dis.* **18**, 650–656 (2018).
14. Y. Barogui, R. C. Johnson, T. S. van der Werf, G. Sopoh, A. Dossou, P. U. Dijkstra, Y. Stienstra, Functional limitations after surgical or antibiotic treatment for Buruli ulcer in Benin. *Am. J. Trop. Med. Hyg.* **81**, 82–87 (2009).
15. E. Marion, A. Chauty, M. Kempf, Y. le Corre, Y. Delneste, A. Croue, L. Marsollier, Clinical features of spontaneous partial healing during *Mycobacterium ulcerans* infection. *Open Forum Infect. Dis.* **3**, ofw013 (2016).
16. D. P. O'Brien, A. Murrie, P. Meggyesy, J. Priestley, A. Rajcoomar, E. Athan, Spontaneous healing of *Mycobacterium ulcerans* disease in Australian patients. *PLOS Negl. Trop. Dis.* **13**, e0007178 (2019).
17. A. Benard, C. Sala, G. Pluschke, *Mycobacterium ulcerans* mouse model refinement for pre-clinical profiling of vaccine candidates. *PLOS ONE* **11**, e0167059 (2016).
18. I. U. Egbuniwe, S. N. Karagiannis, F. O. Nestle, K. E. Lacy, Revisiting the role of B cells in skin immune surveillance. *Trends Immunol.* **36**, 102–111 (2015).
19. S. A. Geherin, S. R. Fintushel, M. H. Lee, R. P. Wilson, R. T. Patel, C. Alt, A. J. Young, J. B. Hay, G. F. Debes, The skin, a novel niche for recirculating B cells. *J. Immunol.* **188**, 6027–6035 (2012).
20. S. A. Geherin, M. H. Lee, R. P. Wilson, G. F. Debes, Ovine skin-recirculating γδ T cells express IFN-γ and IL-17 and exit tissue independently of CCR7. *Vet. Immunol. Immunopathol.* **155**, 87–97 (2013).
21. R. P. Wilson, S. E. McGettigan, V. D. Dang, A. Kumar, M. P. Cancro, N. Nikbakht, W. Stohl, G. F. Debes, IgM plasma cells reside in healthy skin and accumulate with chronic inflammation. *J. Invest. Dermatol.* **139**, 2477–2487 (2019).

22. L. Marsollier, P. Brodin, M. Jackson, J. Korduláková, P. Tafelmeyer, E. Carbonnelle, J. Aubry, G. Milon, P. Legras, J. P. S. André, C. Leroy, J. Cottin, M. L. J. Guillou, G. Reysset, S. T. Cole, Impact of *Mycobacterium ulcerans* biofilm on transmissibility to ecological niches and Buruli ulcer pathogenesis. *PLOS Pathog.* **3**, e62 (2007).
23. C. A. Janeway Jr., P. Travers, M. Walport, M. J. Shlomchik, The major histocompatibility complex and its functions, in *Immunobiology: The Immune System in Health and Disease* (Garland Science, ed. 5, 2001).
24. R. M. Martin, J. L. Brady, A. M. Lew, The need for IgG2c specific antiserum when isotyping antibodies from C57BL/6 and NOD mice. *J. Immunol. Methods* **212**, 187–192 (1998).
25. B. S. Hall, K. Hill, M. McKenna, J. Ogbechi, S. High, A. E. Willis, R. E. Simmonds, The pathogenic mechanism of the *Mycobacterium ulcerans* virulence factor, mycolactone, depends on blockade of protein translocation into the ER. *PLOS Pathog.* **10**, e1004061 (2014).
26. J. Tellier, S. L. Nutt, Standing out from the crowd: How to identify plasma cells. *Eur. J. Immunol.* **47**, 1276–1279 (2017).
27. K. Kassi, K. Kouame, W. Allen, L. A. Kouassi, W. Ance, J. M. Kanga, Squamous cell carcinoma secondary to Buruli ulcer: A clinical case report in a young girl. *Bacteriol. Virusol. Parazitol. Epidemiol.* **55**, 25–28 (2010).
28. E. Minutilli, G. Orefici, M. Pardini, F. Giannoni, L. M. Muscardin, G. Massi, M. Sanguinetti, G. Fadda, D. Di Miceli, G. B. Doglietto, Squamous cell carcinoma secondary to buruli ulcer. *Dermatol. Surg.* **33**, 872–875 (2007).
29. M. Bolz, N. Ruggli, N. Borel, G. Pluschke, M. T. Ruf, Local cellular immune responses and pathogenesis of Buruli ulcer lesions in the experimental *Mycobacterium Ulcerans* pig infection model. *PLOS Negl. Trop. Dis.* **10**, e0004678 (2016).
30. B. Geiger, J. Wenzel, M. Hantschke, I. Haase, S. Ständer, E. von Stebut, Resolving lesions in human cutaneous leishmaniasis predominantly harbour chemokine receptor CXCR3-positive T helper 1/T cytotoxic type 1 cells. *Br. J. Dermatol.* **162**, 870–874 (2010).
31. D. Simon, S. Hösli, G. Kostylina, N. Yawalkar, H. U. Simon, Anti-CD20 (rituximab) treatment improves atopic eczema. *J. Allergy Clin. Immunol.* **121**, 122–128 (2008).
32. K. Yanaba, M. Kamata, N. Ishiura, S. Shibata, Y. Asano, Y. Tada, M. Sugaya, T. Kadono, T. F. Tedder, S. Sato, Regulatory B cells suppress imiquimod-induced, psoriasis-like skin inflammation. *J. Leukoc. Biol.* **94**, 563–573 (2013).
33. N. Nishio, S. Ito, H. Suzuki, K. -I. Isobe, Antibodies to wounded tissue enhance cutaneous wound healing. *Immunology* **128**, 369–380 (2009).
34. N. Abboud, S. K. Chow, C. Saylor, A. Janda, J. V. Ravetch, M. D. Scharff, A. Casadevall, A requirement for FcγR in antibody-mediated bacterial toxin neutralization. *J. Exp. Med.* **207**, 2395–2405 (2010).
35. P. L. De Gentile, C. Mahaza, F. Rolland, B. Carbonnelle, J. L. Verret, D. Chabasse, [Cutaneous ulcer from *Mycobacterium ulcerans*. Apropos of 1 case in French Guiana]. *Bull. Soc. Pathol. Exot.* **85**, 212–214 (1992).
36. K. M. George, D. Chatterjee, G. Gunawardana, D. Welty, J. Hayman, R. Lee, P. L. C. Small, Mycolactone: A polyketide toxin from *Mycobacterium ulcerans* required for virulence. *Science* **283**, 854–857 (1999).
37. E. Marion, S. Prado, C. Cano, J. Babonneau, S. Ghamrawi, L. Marsollier, Photodegradation of the *Mycobacterium ulcerans* toxin, mycolactones: Considerations for handling and storage. *PLOS ONE* **7**, e33600 (2012).
38. S. A. Geherin, D. Gómez, R. A. Glabman, G. Ruthel, A. Hamann, G. F. Debes, IL-10$^+$ innate-like B cells are part of the skin immune system and require α4β1 integrin to migrate between the peritoneum and inflamed skin. *J. Immunol.* **196**, 2514–2525 (2016).
39. K. Pracht, J. Meinzinger, P. Daum, S. R. Schulz, D. Reimer, M. Hauke, E. Roth, D. Mielenz, C. Berek, J. Côrte-Real, H.-M. Jäck, W. Schuh, A new staining protocol for detection of murine antibody-secreting plasma cell subsets by flow cytometry. *Eur. J. Immunol.* **47**, 1389–1392 (2017).


**Acknowledgments:** We thank all members of the SCAHU and PACEM platforms and Lore Dubesset for technical assistance. **Funding:** This work was supported by INSERM, Atip Avenir program, Fondation Raoul Follereau–France, Agence Nationale de la Recherche (ANR) BU_SPONT_HEAL project (InfectEra project) and MYCOPARADOX ANR project, Angers University (REPAIR project), Société Française de Dermatologie, and the Pays de la Loire region (STARTER project). J.M., L.A., and A.A. acknowledge support from the Laboratoire d'Excellence Integrative Biology of Emerging Infectious Diseases (grant no. ANR-10-LABX-62-IBEID) and the ANR under the "Investments for the Future" program (grant no. ANR-10-IAHU-01). A.A. acknowledges support from the Fondation pour la Recherche Médicale (grant no. DMI20091117308). **Author contributions:** M.F., L.A., A.A., and E.M. conceived and designed the experiments. M.F., A.P., J.M., M.R.-S., A.D., L.E., J.-P.S.-A., A.C., and E.M. performed the experiments. M.F., A.P., J.M., F.K., M.R.-S., Y.D., P.J., J.-P.S.-A., A.C., F.A., L.A., A.A., and E.M. performed data analysis. M.F., J.M., F.K., M.R.-S., F.A., Y.D., P.J., L.A., A.A., and E.M. wrote the paper. **Competing interests:** The authors declare that they have no competing interests. **Data and materials availability:** All data needed to evaluate the conclusions in the paper are present in the paper and/or the Supplementary Materials. Additional data related to this paper may be requested from the authors.

Submitted 22 April 2019
Accepted 25 November 2019
Published 26 February 2020
10.1126/sciadv.aax7781

**Citation:** M. Foulon, A. Pouchin, J. Manry, F. Khater, M. Robbe-Saule, A. Durand, L. Esnault, Y. Delneste, P. Jeannin, J.-P. Saint-André, A. Croué, F. Altare, L. Abel, A. Alcaïs, E. Marion, Skin-specific antibodies neutralizing mycolactone toxin during the spontaneous healing of *Mycobacterium ulcerans* infection. *Sci. Adv.* **6**, eaax7781 (2020).